

**Diesel Particulate Matter Induces Toxicity Within *Caenorhabditis elegans* in a Manner  
Distinct from Protein Misfolding**

Jeremiah Joshua Studivant

A thesis submitted to the faculty of the University of the South in partial fulfillment of the  
requirements for honors in the Department of Biology

May 1, 2024

**Diesel Particulate Matter Induces Toxicity Within *Caenorhabditis elegans* in a Manner  
Distinct from Protein Misfolding**

Jeremiah Joshua Studivant

A thesis submitted to the faculty of the University of the South in partial fulfillment of the  
requirements for honors in the Department of Biology

May 1, 2024



Elise Kikis, Ph.D. (thesis advisor)



Chris Shelley, Ph.D. (thesis committee)



Kirk Zigler, Ph.D. (thesis committee)

## Abstract

Neurodegenerative diseases are characterized by the age-dependent failure of the proteostasis network (PN)—a critical regulator of protein folding, trafficking, and degradation—leading to an inability to maintain protein folding homeostasis (proteostasis) and eventually resulting in accelerated loss of neurons. Huntington’s disease (HD) is a neurodegenerative disorder caused by a mutation within the huntingtin gene, encoding an expansion of a glutamine (polyQ) repeat. This polyQ expansion is prone to misfolding, perturbing proteostasis. While significant advances have been achieved in understanding risk factors for neurodegenerative diseases, the impact of air pollution on their progression represents a novel and emerging area of concern. Despite the global prevalence of pollutant exposure, our understanding of its effect on the progression of neurodegenerative diseases is limited. Previous work has demonstrated that nanoparticulate matter (nPM) exacerbates proteostasis failure, increasing polyQ protein toxicity in *C. elegans*. Yet, the variable composition of nPM, influenced by factors such as collection time and geographic location, can result in inconsistent bioactivity assessments for experimental reproduction. Therefore, we began focusing on the effect of a more refined particle, specifically, investigating the effect of commercially available diesel particulate matter (dPM) on proteostasis. To examine proteostasis integrity we employed a *C. elegans* model expressing a polyQ sequence, fused to a yellow fluorescent protein (YFP), as a sensor of the protein folding environment. Surprisingly, we found that dPM induces cellular toxicity in a manner that is independent of polyQ misfolding. Identifying the effect dPM has on proteostasis offers new insight into how nano pollutants may influence the progression of neurodegenerative diseases.

## Table of Contents

<b>Abstract</b>	<b>2</b>
<b>Table of Contents</b>	<b>3</b>
<b>Introduction</b>	<b>4</b>
<b>Methods and Materials</b>	<b>6</b>
<i>C. elegans</i> Strains and Maintenance	6
Table 1. <i>C. elegans</i> Strains	6
Acquiring diesel Particulate Matter	7
Exposure Paradigm	7
Thrashing Assays	7
Aggregation Counting	8
Native Gel Electrophoresis	8
<b>Results</b>	<b>9</b>
Exposure to dPM suppresses Q35::YFP aggregation	9
Figure 1   Exposure to dPM suppresses Q35::YFP aggregation	10
Exposure to dPM is not associated with changes in the amount of oligomers	11
Figure 2   Exposure to dPM is not associated with changes in the amount of oligomers	12
Exposure to dPM increases toxicity in a manner that is independent of polyQ misfolding	13
Figure 3   Exposure to dPM increases toxicity in manner independent of polyQ misfolding	14
<b>Discussion</b>	<b>15</b>
<b>References</b>	<b>18</b>
<b>Acknowledgements</b>	<b>22</b>

## Introduction

Neurodegenerative diseases are characterized by the progressive loss of neurons triggered by the accumulation of toxic misfolded proteins [1]. Huntington's disease (HD) is an autosomal dominant disorder that is caused by an expansion of polyglutamine (polyQ)-encoding CAG repeats in the gene that encodes the huntingtin protein [2]. This PolyQ expansion results in protein misfolding and aggregation, causing neurodegeneration. Likewise, Alzheimer's disease (AD) is characterized by the deposition of amyloid beta ( $A\beta$ ) plaques and neurofibrillary tangles of hyperphosphorylated tau. Thus, both HD and AD are considered diseases of protein conformations [3].

The term proteostasis refers to the maintenance of a healthy proteome. The Proteostasis Network (PN) is composed of nearly 2,000 proteins [4]; some of which are molecular chaperones that coordinate protein folding and other specialized proteins, such as proteases, that are involved in protein degradation. One of the hallmarks of aging and progressive diseases is the failure to maintain proteostasis, which occurs when protein misfolding exceeds the capacity of the cell's molecular chaperones to properly fold proteins. This is known as the buffering capacity and occurs both during normal aging and as a consequence of conformational diseases [5].

Air pollution is the second highest risk factor for noncommunicable diseases [6], causing an estimated 8.34 million deaths per year worldwide [7]. Moreover, exposure to nano-sized particulate matter (nPM), obtained from traffic-derived air pollution, increases  $A\beta$  aggregation in a mouse model of AD expressing an AD-associated mutant form of the human APP gene and the ApoE4 allele, which exacerbates the symptoms of AD [8]. Nano-sized particulate matter is a heterogeneous mixture suspended in the atmosphere due to the burning of diesel, fossil, wood, and gasoline [9], and samples collected at different times and locations may vary considerably in

their makeup and bioactivity. Diesel particulate matter (dPM) consists of more refined compounds, such as elemental carbon, Polycyclic Aromatic Hydrocarbons (PAHs), and nitro-PAHs at its core center. The core center of dPM is highly absorbing, attracting small amounts of metals, sulfates, and nitrates at its surface, further being characterized as highly respirable [10]. Commercially available dPM standards provide a consistent and reproducible source of this pollutant to study its effect on protein misfolding and aggregation. Previous research has demonstrated that dPM elevates the levels of pro-inflammatory cytokines, amyloid beta 42 (A $\beta$ 42), and reactive oxygen species in the brains of mice, thereby enhancing toxicity. [11]. To determine whether dPM disrupts the protein folding environment, we utilized the aggregation-prone protein, PolyQ, fused to a yellow fluorescent protein (YFP), expressed in *C. elegans*' body wall muscle cells, as a sensor of the protein folding environment. At the threshold of aggregation, polyQ35 only aggregates during aging [12] or other conditions under which the load of misfolded proteins is elevated [13]. Because of *C. elegans*' simple gene manipulation techniques and its short life cycle and reproduction, utilizing this model served as an efficient method of monitoring changes in the protein folding environment. Defects in the body wall muscle cells were determined by thrashing assays. Protein aggregation was quantified by visualizing fluorescent foci of YFP. Surprisingly we have found that while dPM is toxic, its effects on muscle cells are independent of protein misfolding.

## Methods and Materials

### *C. elegans* Strains and Maintenance

Strains in Table 1 were obtained from the *Caenorhabditis elegans* Genetics Center (CGC) at the University of Minnesota. Animals were cultured at 15°C on a nematode growth medium (NGM) [14]. OP50 bacteria served as a food source. Animals were age-matched by performing egg lays for 3 h. Egg lays were facilitated by placing 25-30 adult animals on an NGM plate and incubating at 20°C for 3 h, after which the adults were removed.

**Table 1. *C. elegans* Strains**

Strain Name	Genotype	Reference
AM140 unc-Q35::YFP	unc-54p::Q35::YFP::unc-54 3'-UTR (Q35::YFP)	Morely, Brignull et al. 2002
AM140 unc-Q0::YFP	unc-54p::Q0::YFP::unc-54 3'-UTR (YFP)	Morimoto Lab. (n.d.). Retrieved from <a href="https://www.morimoto.org/">https://www.morimoto.org/</a>
N2	Wildtype (Bristol)	Brenner et al. 1974

## **Acquiring diesel Particulate Matter**

Diesel particulate matter (dPM) was purchased from the National Institute of Standards and Technology (NIST). The product number is SRM 1650b. SRM 1650b was prepared from the same bulk diesel particulate material that was issued in 1985 as SRM 1650 [15] and in 2000 as SRM 1650a [16, 17]. Before exposure, each batch of diluted dPM was sterilized by UV-C irradiation in a biosafety cabinet for at least 15 min.

## **Exposure Paradigm**

*C. elegans* were grown to the L4 stage, followed by the exposure of 20-30 animals per well in 96 well plates. Animals were exposed to 25 ng/ml, 75 ng/mL, and 150 ng/mL dPM. M9 medium alone was utilized as the negative control, comprising distilled H<sub>2</sub>O and essential salts. All exposures contained 10 µg/mL cholesterol, and OP50 bacteria. Animals were incubated at 20°C in 96 well plates for 3 d with gentle rocking on a nutator to prevent animals from falling to the bottom of the well.

## **Thrashing Assays**

After the 72 h exposure period, animals were allowed to recover on an NGM plate for 1 h. To measure toxicity in body wall muscle cells, animals were submerged in 10-15 µl of M9 on a glass slide. Following 30 s of recovery, the number of body bends per 30 s was quantified. Assays were performed with a total of 30 animals (n = 30) per genotype per exposure. A total of three biological replicates were performed.

## **Aggregation Counting**

Aggregation was measured in live animals at day 3 of adulthood. After chronic exposure to dPM for 72 h, starting at the L4 stage, animals recovered on an NGM plate for 1 h. After recovery, plates were chilled on ice to limit movement during imaging. Imaging was performed with a Leica M165FC stereomicroscope (Wetzlar, Germany) fitted with an ORCA-Flash 4.0 V3 camera (Hamamatsu Photonics, Japan). The total aggregate number was determined by counting fluorescent foci in each of the 20 animals (n = 20) per genotype per exposure. A total of three biological replicates were performed.

## **Native Gel Electrophoresis**

Extraction of native protein from 50-60 animals was performed by mechanical grinding in liquid nitrogen, followed by the addition of 25  $\mu$ L of ice-cold native lysis buffer. The lysis buffer consisted of 50 mM Tris-HCl pH 7.4, 5 mM MgCl<sub>2</sub>, 0.5% Triton X-100, and 0.2 mM PMSF. Native samples were loaded into a 6% native polyacrylamide gel electrophoresis (PAGE). YFP-tagged proteins were visualized in the gel using a UV light on a BioRad gel-doc imaging system (Hercules, CA). The intensity of bands containing YFP-tagged polyQ protein were quantified with ImageJ software.

## Results

### Exposure to dPM suppresses Q35::YFP aggregation

We know that nPM exacerbates the progression of Q35::YFP aggregates in the body wall muscle cells of *C. elegans* [18]. Given that the nPM was collected from an interstate in California at a specific time, its composition will naturally vary from other samples depending on their collection time and location. Inconsistencies between batches in terms of bioactivity make experimental reproduction difficult. To minimize this variability, we examined the effect of commercially available dPM on proteostasis. We found that increased concentrations of dPM significantly suppress aggregate number compared to M9 (0 ng/mL dPM). Whereas, unexposed animals had an average of 6.66 aggregates per animal. Exposing the animals to 150 ng/mL dPM led to a highly significant decrease in the median number of aggregates when compared to both M9 and 25 ng/mL dPM—showing an average of 2.12 aggregates per animal. Similarly, exposure to 75 ng/mL dPM resulted in a highly significant decrease in aggregate quantity when compared to M9 and 25 ng/mL dPM, with an average of 3.34 aggregates per animal. Exposure to 25 ng/mL dPM revealed an aggregate count proximate to that of M9 (no significant difference). These findings suggest that increased concentrations of dPM suppresses polyQ aggregation, revealing a positive effect on proteostasis (Fig. 1A and B).

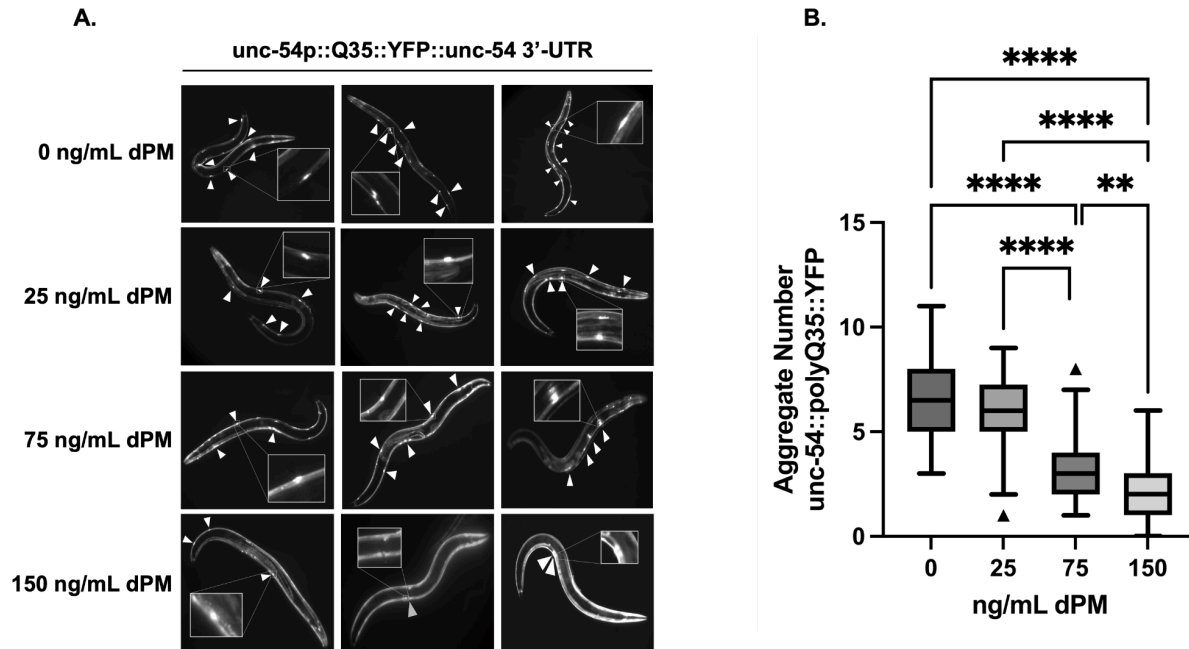


**Figure 1 | Exposure to dPM suppresses Q35::YFP aggregation**

*C. elegans* expressing Q35::YFP in body wall muscle cells were exposed for 3 d to 0 ng/mL, 25 ng/mL, 75 ng/mL, or 150 ng/mL diesel particulate matter (dPM), starting at the L4 stage. **(A)** Fluorescent micrographs of living Q35::YFP animals on NGM plates 3 d after the onset of exposure to dPM or control, 0 ng/mL. Arrows point to focal points of visible aggregates. **(B)** Box plot showing the distribution of Q35::YFP protein aggregates in animals. Sample size (N) = 60 across all conditions. No significant difference is represented by a lack of post hoc comparisons, ‘\*\*\*’ signifies a more significant difference (P-values < 0.01), and ‘\*\*\*\*’ denotes a highly significant difference (P-values < 0.0001) when comparing the average number of aggregates across different dPM concentrations between each exposure. P-values were obtained using a one-way ANOVA test followed by Tukey’s post hoc comparison. The box delineates the 25th-75th percentile (interquartile range (IQR)), with the median represented by the horizontal line. Whiskers extend to the most extreme data points within 1.5 times the IQR. Outliers are individual animals, denoted by triangle symbols (▲).

### **Exposure to dPM is not associated with changes in the amount of oligomers**

To further understand how dPM affects polyQ aggregation, we utilized native gel electrophoresis to distinguish between monomers, oligomers, and large aggregates. The toxic oligomer hypothesis suggests that large-visible aggregates are known to be cytoprotective due to their insoluble phase, while on the contrary, smaller, soluble oligomers are known to be the toxic species [19]. To determine if dPM influences a distinguishable proportion of polyQ35 intermediates, we performed native gel electrophoresis. This technique allowed us to differentiate between the ratio of larger to smaller species of polyQ35 that either resolved to the top of the gel or the bottom of the gel, respectively. Our results show that exposure to dPM had no significant effect on the ratio of high molecular weight species to monomers, indicating that exposure to dPM suppresses the formation of large-visible aggregates while not affecting the presence of polyQ intermediates (Fig. 2A and B). Since toxic, smaller intermediates were indistinguishable between all conditions, we asked whether toxicity were also similar across conditions.

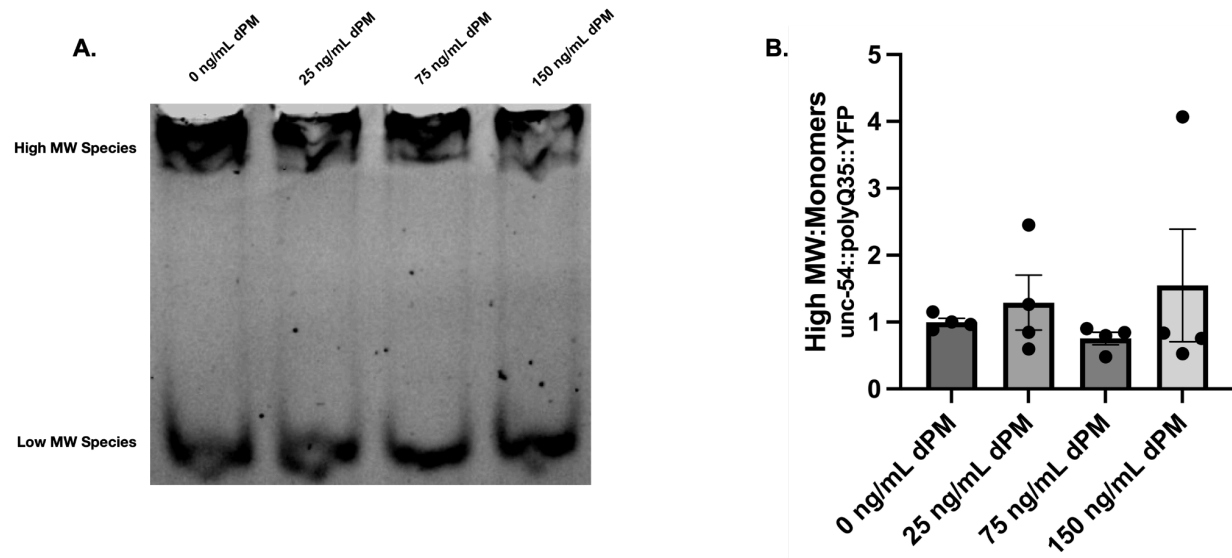


**Figure 2 | Exposure to dPM is not associated with changes in the amount of oligomers**

*C. elegans* expressing Q35::YFP in body wall muscle cells were exposed for 3 d to 0 ng/mL, 25 ng/mL, 75 ng/mL, or 150 ng/mL diesel particulate matter (dPM), starting at the L4 stage. (A) Native gel depicting in-gel Q35::YFP fluorescence with high molecular weight and low molecular weight species. The ratio of the intensity of the two indicated bands was calculated with Image J (B) Bar graph shows the quantification of high molecular weight species relative to monomers as the ratio of the intensity of the two indicated bands in each lane. Bars represent mean values of 4 biological replicates. Individual data points are represented as a circle (●). Error bars represent the standard error of the mean. Welch's t-tests were performed to indicate significant differences. All possible pairwise t-tests were performed and no statistically significant differences were observed.

## **Exposure to dPM increases toxicity in a manner that is independent of polyQ misfolding**

Decreased aggregation is typically associated with decreased proteotoxicity [12, 20, 21]. Thus, we asked whether exposure to dPM had a positive effect on muscle function. To that end, we chronically exposed animals expressing Q35::YFP or YFP protein to either 0 ng/mL or increasing concentrations of dPM for 3 d. As the aggregate-prone protein, polyQ, is expressed in the muscle cells of *C. elegans*, increased aggregation is correlated with decreased motility. Thus, we examined the thrashing rate of animals—number of body bends in liquid per thirty seconds—to changes in muscle function. Surprisingly, after exposure to dPM, motility in animals expressing Q35::YFP was impaired, despite the observed suppression of aggregates. Specifically, an exposure of 150 ng/mL dPM to animals expressing Q35::YFP revealed a significantly decreased thrashing rate compared to animals exposed to 0 and 25 ng/mL dPM. To determine whether the observed toxicity was independent of polyQ misfolding, we employed *C. elegans* expressing the non-aggregated protein, YFP. Similarly to animals expressing Q35::YFP, animals expressing YFP showed a significantly decreased thrashing rate to unexposed controls when exposed to 25, 75, and 150 ng/mL dPM. Both YFP and Q35::YFP slope showed no significant difference. (Fig 3A). To further support these findings animals expressing YFP were imaged for aggregates and showed no visible aggregate in body wall muscle cells (Fig. 3B). Taken together, exposure to dPM results in increased body wall muscle cell toxicity via mechanisms independent of polyQ misfolding.

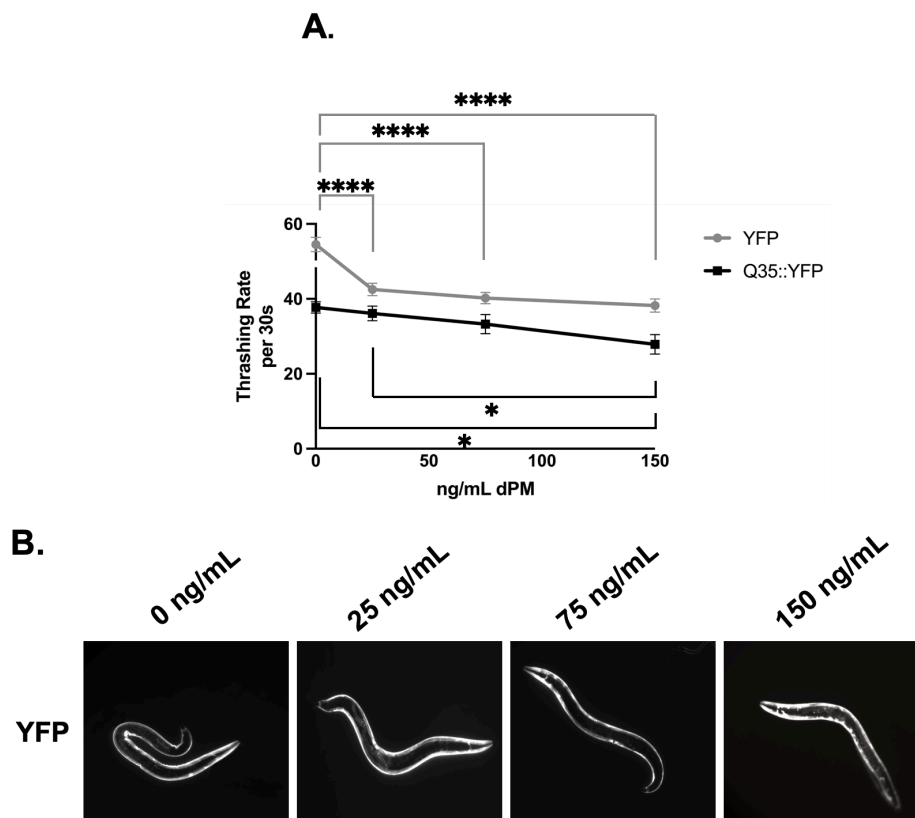


**Figure 3 | Exposure to dPM increases toxicity in manner independent of polyQ misfolding**

*C. elegans* expressing Q35::YFP or YFP in body wall muscle cells were exposed for 3 d to 0 ng/mL, 25 ng/mL, 75 ng/mL, or 150 ng/mL diesel particulate matter (dPM), starting at the L4 stage. **(A)** Line Graph representing the mean thrashing rate of animals expressing Q35::YFP or YFP protein in body wall muscle cells following dPM exposure. Sample size (N) = 30 across all conditions. P-values to measure the difference between YFP and Q35::YFP slopes were obtained using a linear regression test and a one-way ANOVA test followed by Tukey's post hoc comparison to measure the difference between each condition. No significant difference is represented by a lack of post hoc comparisons, "\*" represents a significant difference (P-values < 0.05), and "\*\*\*\*" denotes a highly significant difference (P-values < 0.0001) between each exposure for each genotype. Error bars represent the standard error of the mean (SEM). **(B)** Fluorescent micrographs of living YFP animals on NGM plates 3 d after the onset of exposure to dPM or control, M9.

## Discussion

Here, we described how exposure to an air pollutant, dPM, affects proteostasis. We showed that exposure to dPM suppressed the total number of large-visible aggregates in animals. This study indicates that exposure to dPM has a positive effect on proteostasis. In contrast, in our recent study of nPM's influence on proteostasis, polyQ aggregation increased, revealing that nPM exacerbates proteostasis failure [18]. This difference may be due to the differences in nPM's chemical composition. Subsequently, to understand if dPM had an influence on the proportion of higher to smaller weight polyQ35 oligomers, we utilized native gel electrophoresis and found that the ratio of high molecular weight to monomer species were unchanged in response to dPM, suggesting that exposure to dPM is not associated with the increased or decreased amount of polyQ35 oligomers.

In the native gel electrophoresis analysis, two samples at concentrations of 25 ng/mL and 150 ng/mL dPM exhibited unusual high levels of larger, high molecular weight (HW) aggregates relative to monomers, significantly deviating from the group mean (Fig. 2B). These outliers may be a result of an actual biological effect where a particular sample had a significantly higher ratio of HW to oligomer species, or simply a result of errors during the electrophoresis methodology. Furthermore, the integrity of protein aggregates and their interactions are crucial in assessing their size and composition via native gel electrophoresis. For instance, it is conceivable that the process of lysing the *C. elegans* might inadvertently promote further aggregation of polyQ species, thus altering the native aggregation state present within the cells. However, to mitigate these effects, the use of liquid nitrogen and ice throughout the sample preparation process acted to retard the kinetics of protein interactions, thereby, persevering the in vivo state of the polyQ aggregates.

Additionally, the lysis buffer included a mild detergent designed to solubilize proteins, thereby maintaining the native structure of proteins during analysis.

In addition, exposure to dPM exerts a generalized toxic effect on animals expressing YFP in body wall muscle cells—as indicated by decreased muscle function via thrashing assays—showing that its effects are independent of protein misfolding. The toxic effects of exposure to dPM were observed to increase mortality in animals at higher concentrations. However, for the purpose of this study, only the experimental results where the population remained consistent throughout the exposure period were considered. This method may be selected for individuals less susceptible to dPM-induced aggregation, as those with rapid aggregation onset was not accounted for in experimental data due to early death.

Given that misfolded proteins cause proteotoxic stress, our findings reveal that dPM-induced cellular toxicity is independent of polyQ misfolding. The generalized toxicity arising from exposure to dPM could be the result of a damage not related to protein folding within the cell. It has been shown that dPM induces increased inflammation, neuro-inflammation, DNA damage, up-regulation of neurodegenerative disease markers, and oxidative stress in various tissues of the rat brain, further leading to neurodegeneration [11, 22]. In fact, the presence of these cellular stresses could induce the upregulation of molecular chaperones, which may further increase the buffering capacity to maintain proteostasis. A crucial next step in understanding the suppression of polyQ aggregation is to utilize qRT-PCR to investigate transcription factors responsible for inducing more chaperone transcripts. To further investigate increased inflammation, we can test for an increase in markers such as cytokines and/or NLR family pyrin domain containing 3 (NLRP3), a vital protein for the induction of cellular inflammation [23].

Our study elucidates dPM's positive effect on proteostasis by revealing its suppression in polyQ aggregates. In addition, dPM's toxicity to the cell is induced via mechanisms independent of protein misfolding. Understanding the dynamic effect dPM induces on proteostasis may alleviate major health risks associated with the progression of neurodegenerative diseases.

## References

1. Camandola, S., & Mattson, M. P. (2017, April 24). *Brain metabolism in health, aging, and neurodegeneration* | *The EMBO Journal*. Brain metabolism in health, aging, and neurodegeneration. <https://doi.org/10.15252/emboj.201695810>
2. MacDonald, Marcy E., Ambrose, Christine M., Duyao, Mabel P., Myers, Richard H., Lin, Carol, Srinidhi, Lakshmi, Barnes, Glenn, Taylor, Sherryl A., James, Marianne, Groot, Nicolet (1993, March 26). A novel gene containing a trinucleotide repeat that is expanded and unstable on Huntington's disease chromosomes. *Cell* 72(6): 971-983.  
[http://dx.doi.org/10.1016/0092-8674\(93\)90585-E](http://dx.doi.org/10.1016/0092-8674(93)90585-E)
3. Carrell, R. W., & Lomas, D. A. (1997, July 12). *Conformational disease - the lancet*. Conformational disease. [https://doi.org/10.1016/S0140-6736\(97\)02073-4](https://doi.org/10.1016/S0140-6736(97)02073-4)
4. Hipp, M. S., Kasturi, P., & Hartl, F. U. (2019, February 7). The proteostasis network and its decline in ageing. *Nature reviews. Molecular cell biology*, 20(7), 421–435.  
<https://doi.org/10.1038/s41580-019-0101-y>
5. Labbadia, J., & Morimoto, R. I. (2015, March 12). The biology of proteostasis in aging and disease. *Annual review of biochemistry*, 84, 435–464.  
<https://doi.org/10.1146/annurev-biochem-060614-033955>
6. World Health Organization. (n.d.). *Ambient (outdoor) Air Pollution*. World Health Organization.  
[https://www.who.int/news-room/fact-sheets/detail/ambient-\(outdoor\)-air-quality-and-health](https://www.who.int/news-room/fact-sheets/detail/ambient-(outdoor)-air-quality-and-health)

7. Lelieveld J, Haines A, Burnett R, Tonne C, Klingmüller K, Münzel T et al. (2023, November 23). Air pollution deaths attributable to fossil fuels: observational and modelling study *BMJ* 2023; 383 :e077784. <https://doi.org/10.1136/bmj-2023-077784>
8. Cacciottolo, M., Wang, X., Driscoll, I., Woodward, N., Saffari, A., Reyes, J., Serre, M. L., Vizuete, W., Sioutas, C., Morgan, T. E., Gatz, M., Chui, H. C., Shumaker, S. A., Resnick, S. M., Espeland, M. A., Finch, C. E., & Chen, J. C. (2017, January 31). Particulate air pollutants, APOE alleles and their contributions to cognitive impairment in older women and to amyloidogenesis in experimental models. *Translational psychiatry*, 7(1), e1022. <https://doi.org/10.1038/tp.2016.280>
9. Patricia Sierra-Vargas, M., & Teran, L. M. (n.d.). *Air pollution: Impact and prevention*. Wiley Online Library. <https://onlinelibrary.wiley.com/doi/10.1111/j.1440-1843.2012.02213.x>
10. Wichmann H. E. (2008, October 20). Diesel exhaust particles. *Inhalation toxicology*, 19 Suppl 1, 241–244. <https://doi.org/10.1080/08958370701498075>
11. M. Durga, T. Devasena, A. Rajasekar. (2015, September). Determination of LC50 and sub-chronic neurotoxicity of diesel exhaust nanoparticles. <https://doi.org/10.1016/j.etap.2015.06.024>.
12. Morley, J. F., Brignull, H. R., Weyers, J. J., & Morimoto, R. I. (2002, July 16). The threshold for polyglutamine-expansion protein aggregation and cellular toxicity is dynamic and influenced by aging in *Caenorhabditis elegans*. *Proceedings of the National Academy of Sciences of the United States of America*, 99(16), 10417–10422. <https://doi.org/10.1073/pnas.152161099>

13. Rao, R. V., & Bredesen, D. E. (2004, December 16). Misfolded proteins, endoplasmic reticulum stress and neurodegeneration. *Current opinion in cell biology*, 16(6), 653–662.  
<https://doi.org/10.1016/j.ceb.2004.09.012>
14. Brenner S. (1974, May 1). The genetics of *Caenorhabditis elegans*. *Genetics*, 77(1), 71–94. <https://doi.org/10.1093/genetics/77.1.71>
15. *Diesel Particulate Matter*. Shop nist. (n.d.).  
[https://shop.nist.gov/ccrz\\_\\_ProductDetails?sku=1650b&store=DefaultStore&cclcl=en\\_US](https://shop.nist.gov/ccrz__ProductDetails?sku=1650b&store=DefaultStore&cclcl=en_US)
16. SRM 1650; Diesel Particulate Matter; National Institute of Standards and Technology; U.S. Department of Commerce: Gaithersburg, MD (1985).
17. SRM 1650a; Diesel Particulate Matter; National Institute of Standards and Technology; Department of Commerce: Gaithersburg, MD (2000).
18. Manriquez B., A., Papapanagiotou J. A., Strysick C. A., Green E. H., Kikis, E. A . (2023, February 23). Nanoparticulate air pollution disrupts proteostasis in *Caenorhabditis elegans*. *PLOS ONE*. <https://doi.org/10.1371/journal.pone.0275137>
19. Verma M, Vats A, Taneja V. (2015, June 18) Toxic species in amyloid disorders: Oligomers or mature fibrils. *Ann Indian Acad Neurol*. [10.4103/0972-2327.144284](https://doi.org/10.4103/0972-2327.144284)
20. Drummond DA, Wilke CO. (2008, July 25) Mistranslation-induced protein misfolding as a dominant constraint on coding-sequence evolution. *Cell*. [10.1016/j.cell.2008.05.042](https://doi.org/10.1016/j.cell.2008.05.042)
21. Ben-Zvi A., Miller E.A., and Morimoto R.I. (2009, September 1). Collapse of proteostasis represents an early molecular event in *Caenorhabditis elegans* aging.  
<https://doi.org/10.1073/pnas.0902882106>

22. Kipen H, Rich D, Huang W, Zhu T, Wang G, Hu M, Lu SE, Ohman-Strickland P, Zhu P, Wang Y, Zhang JJ. (2010, August 12). Measurement of inflammation and oxidative stress following drastic changes in air pollution during the Beijing Olympics: a panel study approach. *Ann N Y Acad Sci.* [10.1111/j.1749-6632.2010.05638.x](https://doi.org/10.1111/j.1749-6632.2010.05638.x)
23. Missiroli, S., Patergnani, S., Caroccia, N. *et al.* (2018, February 28) Mitochondria-associated membranes (MAMs) and inflammation. *Cell Death Dis* 9, 329. <https://doi.org/10.1038/s41419-017-0027-2>

## Acknowledgements

As I embark on my scientific journey exploring the natural world, I am immensely grateful to my PI advisor, Dr. Elise A. Kikis. Her mentorship has profoundly deepened my inquisitiveness and drive to understand molecular aspects of biology. I owe an endless debt of gratitude to her for inspiring my intense scientific pursuits.

I also extend my thanks to my supportive lab members: Bailey A. Garcia Manriquez, Julia A. Papapanagiotou, Claire A. Stryck, Ellen Woodward, Hannah Talbott, Hannah Womble, McNoriel Baldonado, and Laine Prince, who have been invaluable throughout various lab experiments and meetings. In addition, thanks to the Summer Undergraduate Research Fellowships for allowing me to investigate my research of exposure to diesel particulate matter during the summer of 2022.

My undergraduate experience has also been greatly enriched by several biology professors at Sewanee. I am thankful to Dr. Kirk S. Zigler for his mentorship; Mrs. Dr. Bethel S. Seballos for her support, the engaging natural philosophy discussions, and helping me regain my purpose after a challenging sophomore year; and Dr. Clint Smith who also played a key role in this process. I am also thankful to Dr. Chris Shelly for the engaging discussions both scientifically and humorously; Dr. Cameron World for providing an engaging space; Dr. Kristen K. Cecala, who kindly assisted during a small moment of need; Dr. Deborah A. McGrath for encouraging my pursuit of biology; Dr. Jonathan P. Evans, who expanded my view and awareness of the natural world; a supportive mentor, Kataren J. Ray for making Sewanee feel like home; and Dr. Kevin Rodriguez for his friendship.

Additional thanks go to the biology faculty members who have shaped my experiences and thinking, including Dr. Pepe Iriarte-Diaz, Dr. Katie E. McGhee, Dr. Grady Wells, and Dr. Matt Schrader.

In the Chemistry Department, I am grateful to Dr. Robert E. Bachman and Professor Justin D. Marsee for allowing me to audit their Thermodynamics and Kinetics lecture; Dr. Rongson Pongdee for his patience in the organic chemistry lab; Dr. Evan E. Joslin for the one-on-one extensive tutoring in her organic chemistry course; Dr. Deon T. Miles for welcoming me to department seminars; Mr. Dr. Leo Seballos for his support during general chemistry, and last but certainly not least, Dr. Richard G. Summers for the evolutionary conversations related to certain biochemical topics within the Advanced Biochemistry lecture.

From the Physics Department, I extend a special thanks to Professor Stephen S. Hancock for enlightening discussions that have sparked my interest for the electrome, which is the totality of all ionic and electrical properties of an organism.

In the Music Department, my advisor, Dr. Stephen Ray Miller provided invaluable support during difficult times—serving as an important figure for my success and well being; Professor Prakash C. Wright for his patience in expanding my intelligence of music theory; and I thank my orchestra directors, Dr. Tiffany Lu and Dr. Mario Alejandro Torres, for their nurturing guidance and support.

Lastly, I would like to express my gratitude to the faculty of the Mathematics, Data Science, Environmental Studies, and Philosophy Department for their guidance. Special thanks to Dr. Doug Drinen who fostered a cherished friendship. I am also grateful to my 'Find Your Place' professor, Dr. Eric Ezell, for the wonderful class readings and discussions during our hikes. Finally, I am thankful to Dr. Matthew Rudd, Joe Brew, Ben Brew, and importantly, Dr. Jim Peterman who introduced me to the world of coding—an experience that had an influence on my path towards investigating the spectacular world of molecular biology.

